

Intrinsic evolutions of dielectric function and electronic transition in tungsten doping Ge₂Sb₂Te₅ phase change films discovered by ellipsometry at elevated temperatures

S. Guo, X. J. Ding, J. Z. Zhang, Z. G. Hu, X. L. Ji, L. C. Wu, Z. T. Song, and J. H. Chu

Citation: [Applied Physics Letters](#) **106**, 052105 (2015); doi: 10.1063/1.4907647

View online: <http://dx.doi.org/10.1063/1.4907647>

View Table of Contents: <http://scitation.aip.org/content/aip/journal/apl/106/5?ver=pdfcov>

Published by the [AIP Publishing](#)

Articles you may be interested in

[Effects of germanium and nitrogen incorporation on crystallization of N-doped Ge_{2+x}Sb₂Te₅ \(x=0,1\) thin films for phase-change memory](#)

[J. Appl. Phys.](#) **113**, 044514 (2013); 10.1063/1.4789388

[Phase change behaviors of Zn-doped Ge₂Sb₂Te₅ films](#)

[Appl. Phys. Lett.](#) **101**, 051906 (2012); 10.1063/1.4742144

[Structural, dynamical, and electronic properties of transition metal-doped Ge₂Sb₂Te₅ phase-change materials simulated by ab initio molecular dynamics](#)

[Appl. Phys. Lett.](#) **101**, 024106 (2012); 10.1063/1.4736577

[A comparative study on electrical transport properties of thin films of Ge₁Sb₂Te₄ and Ge₂Sb₂Te₅ phase-change materials](#)

[J. Appl. Phys.](#) **110**, 013703 (2011); 10.1063/1.3603016

[Optical properties and phase change transition in Ge₂Sb₂Te₅ flash evaporated thin films studied by temperature dependent spectroscopic ellipsometry](#)

[J. Appl. Phys.](#) **104**, 043523 (2008); 10.1063/1.2970069

The advertisement features a row of computer monitors in a library setting, each displaying the cover of the journal 'Computing in Science & Engineering'. The covers show colorful, abstract patterns. In the bottom right corner, the journal's logo is displayed. Below the monitors, the text reads: 'AIP's JOURNAL OF COMPUTATIONAL TOOLS AND METHODS. AVAILABLE AT MOST LIBRARIES.'

computing
IN SCIENCE & ENGINEERING

AIP's JOURNAL OF COMPUTATIONAL TOOLS AND METHODS.
AVAILABLE AT MOST LIBRARIES.

Intrinsic evolutions of dielectric function and electronic transition in tungsten doping $\text{Ge}_2\text{Sb}_2\text{Te}_5$ phase change films discovered by ellipsometry at elevated temperatures

S. Guo (郭爽),¹ X. J. Ding (丁小娟),¹ J. Z. Zhang (张金中),¹ Z. G. Hu (胡志高),^{1,a)} X. L. Ji (纪兴龙),² L. C. Wu (吴良才),² Z. T. Song (宋志棠),² and J. H. Chu (褚君浩)¹

¹Key Laboratory of Polar Materials and Devices, Ministry of Education, Department of Electronic Engineering, East China Normal University, Shanghai 200241, China

²State Key Laboratory of Functional Materials for Informatics, Shanghai Institute of Microsystem and Information Technology, Chinese Academy of Sciences, Shanghai 200050, China

(Received 23 November 2014; accepted 26 January 2015; published online 6 February 2015)

Tungsten (W) doping effects on $\text{Ge}_2\text{Sb}_2\text{Te}_5$ (GSTW) phase change films with different concentrations (3.2, 7.1, and 10.8%) have been investigated by variable-temperature spectroscopic ellipsometry. The dielectric functions from 210 K to 660 K have been evaluated with the aid of Tauc-Lorentz and Drude dispersion models. The analysis of Tauc gap energy (E_g) and partial spectral weight integral reveal the correlation between optical properties and local structural change. The order degree increment and chemical bond change from covalent to resonant should be responsible for band gap narrowing and electronic transition enhancement during the phase change process. It is found that the elevated crystalline temperature for GSTW can be related to improved disorder degree. Furthermore, the shrinkage of E_g for GSTW should be attributed to the enhanced metallicity compared with undoped GST. © 2015 AIP Publishing LLC.

[<http://dx.doi.org/10.1063/1.4907647>]

In the past decades, phase change materials (PCM) such as $\text{GeTe-Sb}_2\text{Te}_3$ chalcogenide compounds have attracted much attention due to their potential application for data storage media.¹ Among this system, $\text{Ge}_2\text{Sb}_2\text{Te}_5$ (GST) alloys have been widely utilized for optical data storage, especially in phase-change random access memory (PRAM), due to their dramatic optical and electrical contrast between amorphous (*a*-GST) and crystalline (*c*-GST) states, and the reversible rapid change between the two phases.² However, with the decrease in the size of PRAM devices, the performances are gradually limited by inadequate properties of GST, e.g., thermal stability, operation speed, and data retention ability. To overcome these notable difficulties, multiple ways have been applied, and one effective method is alien-element doping. It is a remarkable fact that metal doping could improve the recrystallization speed of GST system greatly.³

Tungsten (W) doping GST (GSTW) materials have been investigated due to their elevated crystalline temperature (T_c), phase change speed, data retention ability, and so on. The increased T_c and phase change mechanism (evolutions of crystal structure) have been studied by temperature dependent resistance and Raman scattering measurements. The crystalline structure has been confirmed by transmission electron microscopy (TEM) and X-ray diffraction (XRD). The operation speed of GSTW based PRAM has been significantly improved.^{4,5} Although the structure and electrical properties of pure GST films have been studied,^{6–11} the modification of electronic band structure of GST by W doping has not been well understood up to date. Spectroscopic ellipsometry (SE) is a sensitive measurement method to

characterize thin films and surfaces by dielectric functions.¹²

It is known that the complex dielectric functions are essentially associated with the energy band structure and electronic transitions. Thus, SE is suitable to investigate optical properties and microstructure of phase change materials.

In this letter, W doping and temperature effects on the dielectric functions for GSTW films from amorphous to crystalline phase have been investigated using variable-temperature SE. The abnormal behaviors of electronic band structure and interband transitions with temperature have been discussed in detail.

The GSTW films with a thickness of about 150 nm were prepared by cosputtering pure stoichiometric GST and W on the SiO_2/Si (100) substrates at room temperature. Correspondingly, the undoped GST film with the similar thickness was grown for comparison. Energy dispersive spectrometer (EDS) confirms that the W concentration is around 3.2%, 7.1%, and 10.8% in the GSTW films (GSTW3.2%, GSTW7.1%, and GSTW10.8%). The temperature-dependent SE measurements were performed in the photon energy range of 0.2–4.13 eV (300–6200 nm) at an incident angle of 70° by a vertical variable-angle SE (J. A. Woollam Co., Inc.). The spectral resolution is set to 5 nm, and the measurements were carried out with auto retarder (high accuracy). The samples were mounted into an Instec cell with liquid nitrogen and Janis CRV-217 V with liquid helium as cooling accessories for high and low temperature experiments, respectively. The temperature is various from 210 to 660 K with a precision of about ± 1 K. Note that the window corrections were included as a part of the model during the fitting analysis.

To extract the dielectric functions [$\tilde{\epsilon}(E) = \epsilon_1(E) + i\epsilon_2(E)$] and other significant physical parameters of GSTW films, the ellipsometric spectra were evaluated by a five-layered model

^{a)}Author to whom correspondence should be addressed. Electronic mail: zghu@ee.ecnu.edu.cn. Tel.: +86-21-54345150. Fax: +86-21-54345119.

(air/surface rough layer/GSTW/SiO₂/Si), which were analyzed with the WVASE32 software package. The surface rough layer was defined by effective medium approximation (a mixture of 50% film and 50% void). A single Tauc-Lorentz (TL) oscillator was applied to obtain optical properties of the GSTW films.^{11–13} The TL model can be written as¹⁴

$$\varepsilon_1(E) = \varepsilon_\infty + \frac{2}{\pi} P \int_{E_g}^{\infty} \frac{\xi \varepsilon_2(\xi)}{\xi^2 - E^2} d\xi; \varepsilon_2(E) = \frac{AE_n C(E - E_g)^2 - 1}{(E^2 - E_n^2)^2 + C^2 E^2}, \quad (E \geq E_g)$$

and $\varepsilon_2(E) = 0$, ($E < E_g$), where P is the Cauchy principal part of the integral, ε_∞ is high frequency dielectric constant, and E is incident photon energy. Also, A , E_n , C , and E_g are the amplitude, peak transition energy, broadening term, and Tauc gap energy of the oscillator, respectively. The above TL model follows the Kramers-Krönig transformation (KKT), which has been applied in semiconductors or dielectric materials successfully.^{12,15} A Drude-like term for free carriers was added in infrared (IR) region of 0.2–0.6 eV.^{16–18} The Drude model can be written as: $\varepsilon = -\frac{A_d B_{r_d}}{E^2 + i B_{r_d} E}$, where A_d and B_{r_d} are the amplitude and broadening term of the oscillator, respectively. Note that there is no contribution of free carriers for undoped GST film with amorphous phase.

For example, the experimental and best fitting ellipsometric spectra Ψ and Δ for amorphous (300 K) and crystalline (560 K) GSTW7.1% film are shown in Fig. 1. The absorption edge shows a redshift after crystallization. The best fitting parameters for amorphous (300 K) and crystalline (300 K cooling) GST and GSTW films are given in Table I. Note that the parameters for 300 K cooling were gotten from the ellipsometric spectra as the temperature cooling down to 300 K from 660 K. For all four films, the thickness of surface rough layers (d_s) and films (d_f) obviously decreases after crystallization, which can be attributed to the local order and long-range disorder with the volume expansion in amorphous phase.¹⁹ It is well known that the gradual evolutions of dielectric functions with the increase in temperature are mainly related to the electron-phonon interaction and lattice thermal expansion.²⁰ In order to eliminate the unwanted temperature effects, the best fitting parameters of heating (300 K) and cooling (300 K) stage are extracted. It should be emphasized that the GSTW material

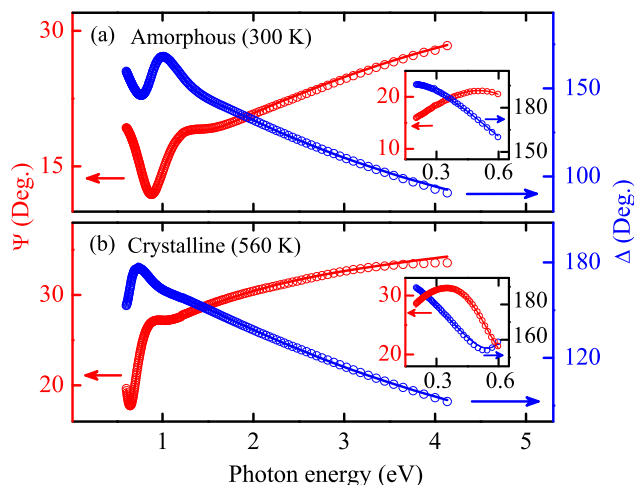


FIG. 1. Experimental (dots) and best fitting (solid lines) ellipsometric spectra of Ψ and Δ for (a) amorphous (300 K) and (b) crystalline (560 K) GSTW7.1% film in UV-vis region of 0.6–4.13 eV, respectively. Note that the insets show the corresponding Ψ and Δ in the IR region of 0.2–0.6 eV.

systems could not restore them back to amorphous phase after heating without a rapid annealing or suitable electrical impulse. With the increase in temperature, the structure of GST transforms from amorphous to face-centered-cubic (FCC) and then to hexagonal (HEX) phase. However, the GSTW changes from amorphous to FCC structure directly.⁴ Therefore, the parameters of GST film at 450 K (FCC) are added for comparison. A good agreement of Tauc gap energy (E_g) in UV-vis and IR regions is presented in Table I. Furthermore, there is a significant shrinkage of Tauc gap energy E_g and peak transition energy E_n for all four samples from amorphous to crystalline structure, which may be caused by the change of long range order (LRO) to medium range order (MRO) of crystalline phase. The broadening parameter C is closely related with the variations in bond angles, lengths, and chemical disorder. A strong suppression of C for the films after crystallization can be observed from Table I, which can be attributed to the change of order degree.^{11,21} The majority of W atoms enter into the crystal lattice, which can be regarded as substitutional impurities. Nevertheless, the crystalline structure will not be seriously affected. Therefore, we speculate that the shrinkage of optical gap energies for W-doped GST films can be explained due to the increase of order degree during the crystallization. The parameter E_g for both amorphous and crystalline films is monotonously decreased with increasing W concentration. GST can be viewed as a compound in the form of (GeTe)₂-Sb₂Te₃. W atoms can substitute Ge or Sb atoms, forming WTe₂ in GST cells. Note that WTe₂ possesses metallicity.²² The E_g can be regarded as zero, which is narrower than that of both GeTe (~0.8 eV) and Sb₂Te₃ (~0.3 eV). Therefore, the E_g can be estimated by the following equation: $E_{gGSTW}^{opt} = xE_{gWTe_2}^{opt} + (1-x)E_{gGST}^{opt} - bx(1-x)$, where x is W doping concentration and b is the bowing parameter. Thus, the band gap narrowing for GSTW should be attributed to the enhanced metallicity compared with undoped GST.²³ The film thickness decreases from 198 to 187 nm during the transition from FCC to HEX geometry of GST film, which can be related to more vacancy in the Ge/Sb layers for FCC than that for HEX phase.¹⁹

Evolutions of the imaginary part (ε_2) for GST and GSTW7.1% films in UV-vis region of 0.6–4.13 eV extracted from ellipsometric measurements are shown in Figs. 2(a) and 2(b), respectively. The broad peaks for ε_2 of *a*-GST and *c*-GST are around 2.2 and 1.4 eV, respectively, which are comparable to the previous data reported.^{11,13,16} The valance band of GST film is dominated by the Ge, Sb, and Te *p* states, and minor contributions from Ge and Sb *s* state. The peaks of ε_2 corresponding to the strong optical absorption are associated with the Te *p* and Sb *p* state electronic transition.¹¹ For GST and GSTW films, the redshift, narrowing, and large enhancement of the main peak for ε_2 from amorphous to crystalline structure can be summarized. Besides, an obvious enhancement of the Drude peaks in IR region for crystalline structure can be found, as shown in the insets of Fig. 2. In particular, the phase change from FCC to HEX structure can be observed by the improvement of Drude contribution in IR region. The significant discrepancy of dielectric functions between amorphous and crystalline phase might be due to the order degree increment of crystalline phase, which is caused by the change of local bonding

TABLE I. Dielectric function parameters of the Tauc-Lorentz and Drude oscillator models for GST and GSTW films are determined from the simulation of ellipsometric spectra. Note that d_s and d_f are the thickness of surface rough layers and films, respectively (a : amorphous, c : crystalline, and 300↓: 300 K cooling).

Samples		GST			GSTW3.2%		GSTW7.1%		GSTW10.8%	
		a	c		a	c	a	c	a	c
Temperature (K)		300	450	300↓	300	300↓	300	300↓	300	300↓
UV-vis (TL) (0.6–4.13 eV)	d_s (nm)	7.43	4.24	1.22	6.04	2.11	5.96	1.93	4.20	1.72
	d_f (nm)	212	198	187	149	138	144	135	140	133
	A (eV)	143	191	154	119	145	106	141	96.5	119
	C (eV)	4.45	1.85	1.64	4.23	1.64	4.34	2.08	4.51	2.18
	E_n (eV)	2.62	1.30	1.28	2.68	1.48	2.85	1.65	2.73	1.69
	E_g (eV)	0.65	0.41	0.37	0.56	0.29	0.45	0.27	0.35	0.23
IR (TL+Drude) (0.2–0.6 eV)	A (eV)	163	272	253	186	197	113	133	117	139
	C (eV)	0.53	2.69	2.56	0.73	2.94	1.42	1.13	2.66	0.76
	E_n (eV)	4.65	1.61	1.44	6.38	5.87	3.89	3.02	3.80	2.69
	E_g (eV)	0.65	0.42	0.37	0.57	0.30	0.44	0.28	0.35	0.24
	A_d (eV)	...	1.94	1.46	1.82	1.93	0.66	1.29	2.85	3.36
	Br_d (eV)	...	1.78	1.65	0.76	2.11	0.75	3.87	1.87	2.57

arrangement from tetrahedral to octahedral coordinated of Ge atoms. It is ultimately dominated by the change of matrix elements corresponding to the intensity of interband transition. The bond characteristics between elements are transformed from covalent bonding for amorphous phase to resonant bonding for crystalline phase. The contribution of resonant bonding should be derived from the relative increase of electronic polarizability, which is a characterization of different dielectric functions between two phases. That is to say, the obvious optical contrast can be attributed to the change of structure and chemical bonding.¹⁶ The vertical shifts shown in Figs. 2(a) and 2(b), expect for the abnormal behavior of GST film transforming from FCC to HEX phase, are obviously from the temperature effects.

To analyze the W doping effects on dielectric functions, the evolutions of ϵ_2 for amorphous (300 K) and crystalline (560 K) GST and GSTW films are shown in Fig. 2(c). The corresponding IR region is shown in the inset. The opposite variation trend of the ϵ_2 peaks from amorphous to crystalline phase for GST and GSTW films can be discovered in UV-vis region. The peaks show a redshift with the increase in W

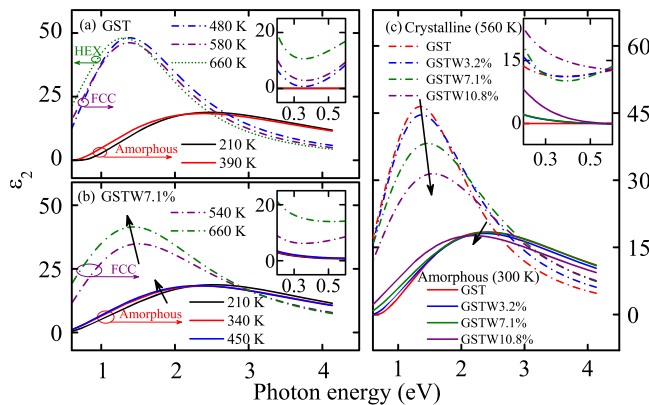


FIG. 2. Evolutions of the imaginary part (ϵ_2) of (a) GST and (b) GSTW7.1% films at several typical temperatures in UV-vis region of 0.6–4.13 eV, respectively. (c) Evolutions of the imaginary part (ϵ_2) of the amorphous (300 K) and crystalline (560 K) GST and GSTW films with different W concentration in UV-vis region of 0.6–4.13 eV. Note that the insets show the corresponding ϵ_2 in the IR region of 0.2–0.6 eV.

concentration for amorphous phase, which can be attributed to the decreased interband transition energy. However, the W dopants lead to a disorder of crystalline phase and inhibit crystallization. The effect can be improved by increasing W concentration, which leads to a blueshift.

To clarify the evolutions of the electronic structure, the Tauc gap energy (E_g) with a function of temperature for GST and GSTW films were plotted in Fig. 3. The variations of E_g for GSTW can be separated into four parts. The analogous Tauc gap energy for GST compared with GSTW can be observed expect for Part II, which can be regarded as an additional part for W doped GST films. Each part was linearly fitted, and the corresponding temperature coefficients (dE_g/dT : k_I to k_{IV}) are shown in Fig. 3. The coefficients of Part I and IV are typical values caused by temperature effects for semiconductors.²⁴ It should be emphasized that the absolute values of k_I are less than that of the corresponding k_{IV} , which can be attributed to the slightly continuous crystallization with increasing temperature. The absolute values of k_{III} are much larger than other values, which can be interpreted by the phase change from amorphous to crystalline phase. Note that the narrowed phase change regions can be related to the

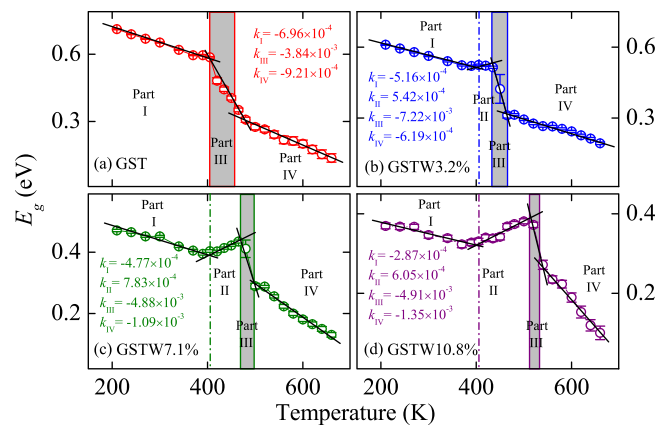


FIG. 3. Tauc gap energy (E_g) evolutions of the GST and GSTW films with different W concentration as a function of temperature. Note that the shadow patterns correspond to the phase change regions. k_I , k_{II} , k_{III} , and k_{IV} are the dE_g/dT values of part I, II, III, and IV, respectively.

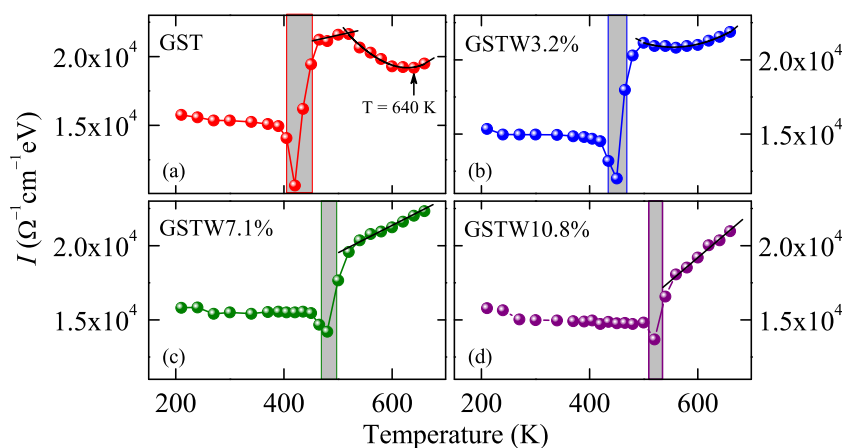


FIG. 4. Partial spectral weight integral (I) evolutions of the GST and GSTW films with different W concentration as a function of temperature in the photon energy region of 0.2–4.13 eV. Note that the shadow patterns correspond to the phase change regions.

acceleratory crystallization with increasing W concentration, which is a significant factor for phase materials. Another abnormal region is Part II for GSTW with the same initial temperature as Part III for GST. The temperature coefficients are positive, which can be attributed to the impurity compensation of donor and p -type semiconductor GST before crystallization. Note that the change between FCC and HEX phase of GST film is modest, which cannot be distinguished from the variations of E_g . With the increase in W concentration, T_c increases from 420 to 520 K, which is similar with the previous data.^{4,5} The phenomenon can be explained by the fact that the heavier W atoms prevent GST elements from further diffusion. The disorder degree of atoms can be improved in GSTW films, which has a contribution to enhance the thermal stability and endurance for GSTW-based PRAM.

To further investigate the Tauc gap narrowing of GST and GSTW films during the crystallization, the partial spectral weight integral (I) evolutions in the photon energy region of 0.2–4.13 eV are shown in Fig. 4. The I can reflect the electrons excited by photons during the selected energy range, which is defined as $I = \int_{E_1}^{E_2} \sigma_1(E) dE$, [$\sigma_1(E) = \epsilon_0 \epsilon_2(E)E$], where $\sigma_1(E)$ is optical conductivity, E_2 and E_1 are the upper and lower bound of the energy range, respectively.²⁵ The parameter I of all four samples decreases gradually in the initial heating stage, which can be ascribed to the thermal activation leading electronic transition with increasing temperature. The I near T_c region decreases first, and then increases sharply, corresponding to the phase change regions Part III obtained in Fig. 3. It is associated with the strong absorption during transition from amorphous to crystalline phase.²⁶ With further increase in temperature, the partial spectral weight integral decreases to a minimum value at 640 K, which can be attributed to the transition from FCC to HEX phase for GST film. The variation trend is suppressed with increasing W doping concentration. It can be related to the fact that further crystallization from FCC to HEX phase is inhibited by the W doping.

In summary, W doping effects on phase change GSTW films have been investigated by temperature dependent SE measurements. The band gap narrowing and electronic transition variation by W doping during phase change process have been confirmed by analyzing dielectric functions.

This work was financially supported by Major State Basic Research Development Program of China (Grant Nos. 2011CB922200 and 2013CB922300), Natural Science

Foundation of China (Grant Nos. 11374097 and 61376129), Projects of Science and Technology Commission of Shanghai Municipality (Grant Nos. 14XD1401500, 13JC1402100, and 13JC1404200), and the Program for Professor of Special Appointment (Eastern Scholar) at Shanghai Institutions of Higher Learning.

- ¹M. Wuttig and N. Yamada, *Nat. Mater.* **6**, 824 (2007).
- ²D. Lencer, M. Salinga, B. Grabowski, T. Hickel, J. Neugebauer, and M. Wuttig, *Nat. Mater.* **7**, 972 (2008).
- ³L. Men, J. Tominaga, H. Fuji, T. Kikukawa, and N. Atoda, *Jpn. J. Appl. Phys., Part 1* **40**, 1629 (2001).
- ⁴X. N. Cheng, F. X. Mao, Z. T. Song, C. Peng, and Y. F. Gong, *Jpn. J. Appl. Phys., Part 1* **53**, 050304 (2014).
- ⁵S. Guo, Z. G. Hu, X. L. Ji, T. Huang, X. L. Zhang, L. C. Wu, Z. T. Song, and J. H. Chu, *RSC Adv.* **4**, 57218 (2014).
- ⁶J. Hegedüs and S. R. Elliott, *Nat. Mater.* **7**, 399 (2008).
- ⁷S. Caravati and M. Bernasconi, *Appl. Phys. Lett.* **91**, 171906 (2007).
- ⁸R. Mazzarello, S. Caravati, S. Angioletti-Uberti, M. Bernasconi, and M. Parrinello, *Phys. Rev. Lett.* **104**, 085503 (2010).
- ⁹T. T. Li, T. H. Lee, S. R. Elliott, and J. R. Abelson, *Appl. Phys. Lett.* **103**, 201907 (2013).
- ¹⁰T. Kato and K. Tanaka, *Jpn. J. Appl. Phys., Part 1* **44**, 7340 (2005).
- ¹¹J. Orava, T. Wágner, J. Šik, J. Příkryl, M. Frumar, and L. Beneš, *J. Appl. Phys.* **104**, 043523 (2008).
- ¹²S. Zhang, J. Z. Zhang, M. J. Han, Y. W. Li, Z. G. Hu, and J. H. Chu, *Appl. Phys. Lett.* **104**, 041106 (2014).
- ¹³P. Fantini, S. Brazzelli, E. Cazzini, and A. Mani, *Appl. Phys. Lett.* **100**, 013505 (2012).
- ¹⁴G. E. Jellison, Jr. and F. A. Modine, *Appl. Phys. Lett.* **69**, 371 (1996); **69**, 2137 (1996).
- ¹⁵Y. J. Cho, N. V. Nguyen, C. A. Richter, J. R. Ehrstein, B. H. Lee, and J. C. Lee, *Appl. Phys. Lett.* **80**, 1249 (2002).
- ¹⁶K. Shportko, S. Kremers, M. Woda, D. Lencer, J. Robertson, and M. Wuttig, *Nat. Mater.* **7**, 653 (2008).
- ¹⁷Y. K. Seo, J.-S. Chung, Y. S. Lee, E. J. Choi, and B. Cheong, *Thin Solid Films* **520**, 3458 (2012).
- ¹⁸A. Mendoza-Galván and J. González-Hernández, *J. Appl. Phys.* **87**, 760 (2000).
- ¹⁹J.-W. Park, S. H. Eom, and H. Lee, *Phys. Rev. B* **80**, 115209 (2009).
- ²⁰A. Dejneka, I. Aulika, V. Trepakov, J. Krepelka, L. Jastrabik, Z. Hubicka, and A. Lymnyk, *Opt. Express* **17**, 14322 (2009).
- ²¹P. Němec, A. Moreac, V. Nazabal, M. Pavlišta, J. Příkryl, and M. Frumar, *J. Appl. Phys.* **106**, 103509 (2009).
- ²²S. L. Tang, R. V. Kasowski, and B. A. Parkinson, *Phys. Rev. B* **39**, 9987 (1989).
- ²³R. Li, Y. F. Jiang, L. Xu, Z. Y. Ma, F. Yang, J. Xu, and W. N. Su, *Phys. Status Solidi A* **210**, 2650 (2013).
- ²⁴J. Šik, J. Hora, and J. Humlíček, *J. Appl. Phys.* **84**, 6291 (1998).
- ²⁵M. A. Majidi, E. Thoeng, P. K. Gogoi, F. Wendt, S. H. Wang, I. Santoso, T. C. Asmara, I. P. Handayani, P. H. M. van Loosdrecht, A. A. Nugroho, M. Rübhausen, and A. Rusydi, *Phys. Rev. B* **87**, 235135 (2013).
- ²⁶D. Franta, M. Hrdlicka, D. Necas, M. Frumar, I. Ohlídal, and M. Pavlišta, *Phys. Status Solidi C* **5**, 1324 (2008).